Sound Source Reconstruction Using Inverse BEM

Article · June 2001

Source: CiteSeer

CITATIONS
18

READS
305

2 authors:

Andreas Schuhmacher
Brüel & Kjaer Sound & Vibration Measurement A/S
21 PUBLICATIONS **323** CITATIONS
SEE PROFILE

Per Christian Hansen
Technical University of Denmark
222 PUBLICATIONS **23,172** CITATIONS
SEE PROFILE

inter·noise 2001
The Hague, Holland
The 2001 International Congress and Exhibition on Noise Control Engineering
The Hague, The Netherlands, 2001 August 27-30

Sound Source Reconstruction Using Inverse BEM

Andreas P. Schuhmacher
Brüel & Kjær Sound and Vibration Measurements A/S
Skodsborgvej 307, DK-2850 Nærum, Denmark

Per Christian Hansen
Informatics and Mathematical Modelling
Technical University of Denmark, DK-2800 Lyngby, Denmark

Abstract

Sound source reconstruction based on boundary element modelling (BEM) and inverse methods has become a powerful tool for noise source identification involving arbitrarily shaped sources. Since the numerical treatment results in a linear discrete ill-posed problem, regularisation must be applied to avoid unstable solutions dominated by noise and errors in the acoustic field data. The key to a useful reconstruction is a method for choosing the optimal amount of regularisation, in order to compute a solution which is based on maximum exploitation of the available information in the given data. Two parameter-choice strategies are compared for a practical test case using a real tyre.

1. Introduction

Inverse BEM is an approach joining acoustic boundary element modelling (BEM) with inverse methods to solve an inverse acoustic source problem. The objective is to compute the unknown surface velocity distribution on a complex acoustic source from measured acoustic field data. Hence, inverse BEM can be seen as general 3-D acoustic holography compared to traditional Near-field Acoustic Holography (NAH) which, in its simplest form, relies on plane geometry as implemented in B&K STSF [1].

In order to apply inverse BEM, a so-called discrete ill-posed problem must be solved after forming a transfer matrix relating the normal surface velocity at boundary nodes to the acoustic pressure at field points. How to form this transfer matrix will be described briefly using an indirect variational formulation, but it could be accomplished in a similar way using a direct boundary element formulation [2,3]. Having established a transfer matrix, the next step is to solve a discrete ill-posed problem. In this paper this is done by means of Tikhonov regularisation where the regularisation parameter is estimated using a parameter-choice method. We describe two different parameter-choice methods, which do not require any information about the contaminating errors in the field pressures. Finally, a test case using real measured data will reveal the robustness of each of these parameter-choice methods.

2. The Discrete Ill-Posed Problem

The acoustic field can be expressed in terms of a double-layer distribution on a surface S:

$$p(P) = \int_S \mu(Q) \frac{\partial G(P,Q)}{\partial \mathbf{n}_Q} dS(Q), \tag{1}$$

where $p(P)$ is the acoustic pressure at field point P, $\mu(Q)$ is the double-layer distribution, $G(P,Q)$ is Green's function, and $\mathbf{n}_Q$ is a normal vector at Q pointing into the exterior region.

The link between the normal surface velocity v_n and the double-layer potential μ is provided by computing the normal derivative of Eq. (1) for a point P on the surface:

$$-j\omega\rho\, v_n(P) = \int_S \mu(Q) \frac{\partial^2 G(P,Q)}{\partial \mathbf{n}_P \partial \mathbf{n}_Q} dS(Q). \tag{2}$$

The quantities ω and ρ are angular frequency and fluid density, respectively.

If we consider m points situated in the exterior region and n boundary nodes of the BEM formulation on the discretised surface, we can discretise Eqs. (1) and (2) to obtain:

$$\mathbf{p} = \mathbf{G}\boldsymbol{\mu} \quad , \quad -j\omega\rho\, \mathbf{B}\mathbf{v}_n = \mathbf{Q}\boldsymbol{\mu}. \tag{3}$$

Here $\mathbf{p}$ is an m-vector with pressures, while $\boldsymbol{\mu}$ and $\mathbf{v}_n$ are n-vectors with nodal values of double-layer potential and normal surface velocity, respectively. In order to discretise Eq. (2) a variational principle is associated with the equation to treat the second derivative of Green's function. The two matrices $\mathbf{B}$ and $\mathbf{Q}$ are symmetric and of size $n \times n$; $\mathbf{B}$ is real-valued whereas $\mathbf{Q}$ is complex. In general, $\mathbf{G}$ is a rectangular complex matrix of size $m \times n$, and we will assume that the number of field points m is greater than or equal to the number of boundary nodes n.

Combining the two matrix-vector expressions in Eq. (3) allows us to express the pressure field in terms of normal surface velocity as

$$\mathbf{p} = -j\omega\rho\, \mathbf{G}\mathbf{Q}^{-1}\mathbf{B}\mathbf{v}_n = \mathbf{H}\mathbf{v}_n. \tag{4}$$

Since Eq. (4) represents a discrete ill-posed problem [4], we can not compute the unknown vector of surface velocities by means of a standard solution approach, because the solution is unstable – i.e., very sensitive to perturbations of the data. Instead, we must employ special stabilisation (regularisation) techniques aiming at solving Eq. (4) in a near-by sense.

3. Tikhonov Regularisation

The condition number of the matrix $\mathbf{H}$ measures the solution's sensitivity to perturbations in the matrix itself as well as in the right-hand side. When we are dealing with ill-conditioned matrices, this condition number is very large. As a consequence, if Eq. (4) is solved naively then a very oscillating solution with a huge norm is obtained due to the unavoidable errors in the right-hand side $\mathbf{p}$. One way of suppressing the disastrous influence of these errors is to solve the initial ill-conditioned problem in a near-by sense with a side constraint on the size of the sought solution. The solution size, in turn, is linked to the solution smoothness, because smooth solutions will have a reasonable size when measured by an appropriate norm. In mathematical form, we can write this as a minimisation problem where the function to be minimised involves a residual norm and a discrete smoothing norm, here based on 2-norms:

$$\min_{\mathbf{v}_n} \left\{ \left\| \mathbf{H}\mathbf{v}_n - \mathbf{p} \right\|_2^2 + \lambda^2 \left\| \mathbf{L}\mathbf{v}_n \right\|_2^2 \right\} \tag{5}$$

The regularisation parameter λ is the only input when a suitable regularisation matrix $\mathbf{L}$ has been defined. In our case studies, $\mathbf{L}$ has been chosen to reflect an area weighting of the unknown boundary values.

If $\lambda = 0$ then we obtain the least-squares problem and an unregularised solution is computed. On the other hand, a large λ favours a small solution size at the cost of a large residual norm. Hence, λ controls the degree with which the regularised solution should fit to the data in $\mathbf{p}_f$ or have small solution size. Clearly, solving Eq. (5) involves a trade-off between the residual norm and the solution size, and this is determined by the single parameter λ. This form of regularisation is known as Tikhonov regularisation, which is discussed at length, e.g., in [4].

4. Parameter-Choice Methods

Choosing the continuous parameter λ in Tikhonov regularisation is not straightforward. Ideally, we would like to determine the regularisation parameter such that the computed regularised solution provides the best possible estimate of the underlying exact solution. The only problem is that the exact solution is not available. Parameter-choice methods should compute regularisation parameters, which are good approximations to the optimal ones.

Methods which do not require information about the norm of the error-vector contaminating **p** are preferred, whenever reliable information about this error-vector is not available. Here we consider two such methods for extracting an optimum regularisation parameter. The first method, which is very popular, is called generalised cross-validation (GCV). It is based on the philosophy that an arbitrary element of the right-hand side should be predicted well by the regularised solution, when this element is left out of the inverse problem. This method works well if the noise is spatially white, i.e., if the elements of the noise vector are unbiased and have the same variance.

Another approach to estimating the regularisation parameter in Tikhonov regularisation is the so-called L-curve criterion. The idea behind the L-curve criterion is to plot the discrete smoothing norm of the regularised solution $\mathbf{v}_n^{\lambda}$ versus the residual norm in a log-log scale, for all valid regularisation parameters. The smoothing norm is here $\left\|\mathbf{L}\,\mathbf{v}_n^{\lambda}\right\|_2$ and the residual norm is $\left\|\mathbf{H}\,\mathbf{v}_n^{\lambda} - \mathbf{p}\right\|_2$, i.e., the two terms occurring in Tikhonov's method. The resulting curve will often have an L-shaped appearance, and hence it is referred to as the L-curve. The horizontal part of the curve is characterised by solutions that have been smoothed too much (over-regularised), while the vertical part is characterised by solutions dominated by the effects of errors (under-regularised). Between these parts, we find solutions representing a balance between fitting the solution to data and keeping the solution's smoothing norm small. The optimum value of the regularisation parameter defined by the L-curve criterion is at the corner of the curve, where we find a solution that has a reasonably small residual as well as a reasonably limited smoothing norm. We emphasise that this is only possible in a plot in log-log scale [5].

5. Results for Tyre Measurements

A real tyre structure on a drum is studied for two different measurement configurations. The tyre is a standard tyre for passenger's cars and its characteristics as a source are investigated in case of a standing tyre excited by a shaker and a rolling tyre at 80 km/h.

The measurements were recorded using a linear microphone array for the tyre side measurement and a circular (curved) array for close measurements at the front and the rear of the tyre. Moreover, four reference microphones were distributed around the tyre in order to derive a principal component description of the sound field. Two of these four reference microphones were placed on the ground in front of and behind the tyre, while the other two microphones were located in the air above the tyre.

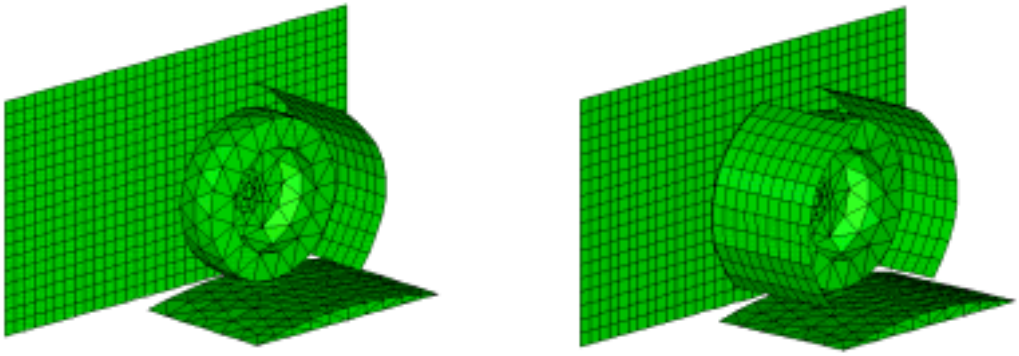

Figure 1. Plane and curved array meshes relative to the boundary element mesh of the tyre/drum; standing tyre (left) and rolling tyre (right).

We used 821 measurement positions for the shaked tyre and 977 for the rolling tyre. The measurement positions relative to the tyre structure are shown in Fig. 1 where the source for reconstruction is modeled as the tyre attached to the drum part. The tyre/drum model is meshed using triangular elements with a total of 371 boundary nodes. For those nodes belonging to the drum part we impose zero surface velocity meaning that only the 266 nodes which belong to the tyre surface are used as unknowns when solving the inverse problem. The transfer matrix is then of size 821×266 for the standing tyre excited by the shaker and 977×266 for the rolling tyre. A fully reflecting infinite plane is included in the tyre/drum model when setting up the problem.

Since four reference microphones are used to derive a principal component description of the sound field, four different pressure fields must be processed by the inverse BEM algorithm. Hence, for each principal component we must estimate the optimal regularisation parameter either by the L-curve criterion or by the GCV method. Finally, we compute the total field by adding the principal fields on an energy basis.

We will specifically analyse the measurement data at 100 Hz for the shaked tyre and at 60 Hz for the rolling tyre. The L-curves corresponding to the first principal component for the two set-ups are plotted in Fig. 2. The regularisation parameter computed by the L-curve criterion and the GCV method are shown on the plots. Clearly, the regularisation parameter computed by the GCV method is too small. This is true for the other principal components as well.

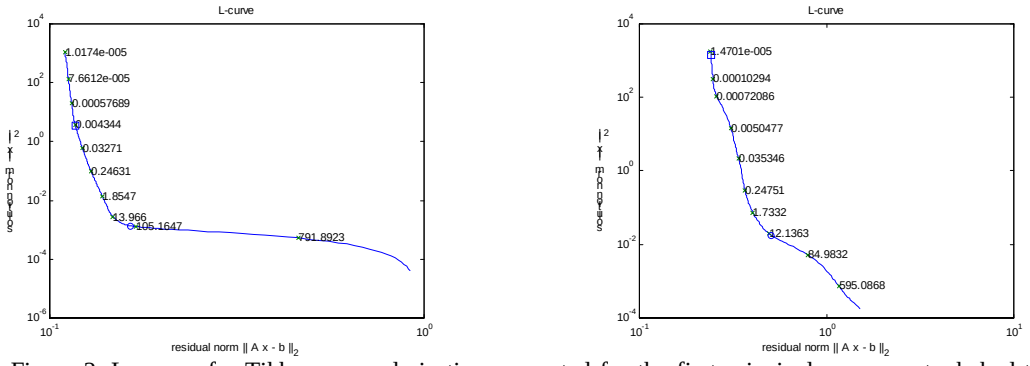

Figure 2. L-curves for Tikhonov regularisation computed for the first principal component; shaked tyre at 100 Hz (left) and rolling tyre at 60 Hz (right). The optimum regularisation parameters computed by the L-curve criterion (circle) and the GCV method (square) are shown.

The total reconstructed surface velocity on the tyre as computed by the L-curve criterion is

shown in Fig. 3. In order to obtain these plots we applied a Wiener filtering of the principal components, corresponding to a smooth cut-off at 15 dB below the largest principal auto-power value. This will avoid poorly estimated principal components blurring the total calculated field.

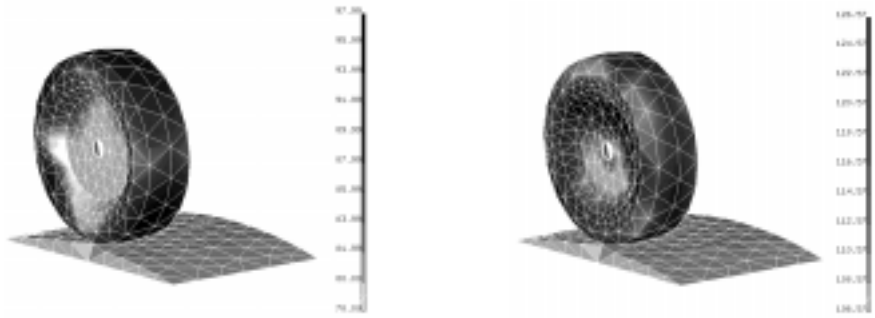

Figure 3. Reconstructed surface velocity (dB) on the tyre usingthe L-curve criterion; standing tyre at 100 Hz (left) and rolling tyre at 60 Hz (right).

6. Comparison with Near-Field Acoustic Holography

For both measurements, we can process the data recorded at the tyre-side with the aid of NAH as implemented in B&K STSF. By doing so, we are able to reconstruct the sound field on a plane surface closer to the tyre-side than the measurement plane. Thus, we can compare the reconstructions obtained by the inverse BEM approach with results from STSF. In order to do so, the reconstructed surface velocity distribution on the tyre surface is applied as boundary condition in a forward BEM problem for computing sound field parameters on a reference plane close to the tyre-side, coinciding with the plane used in the STSF calculations.

In Figs. 4 and 5, the sound pressure and the normal particle velocity are computed on the reference surface located 2 cm from the tyre side. In the STSF technique, the measurement data collected on the measurement plane 7 cm from the tyre must be back propagated 5 cm onto the reference surface. When using inverse BEM, the computed tyre surface velocity is used as input in a forward BEM problem for computing the sound field at the reference plane.

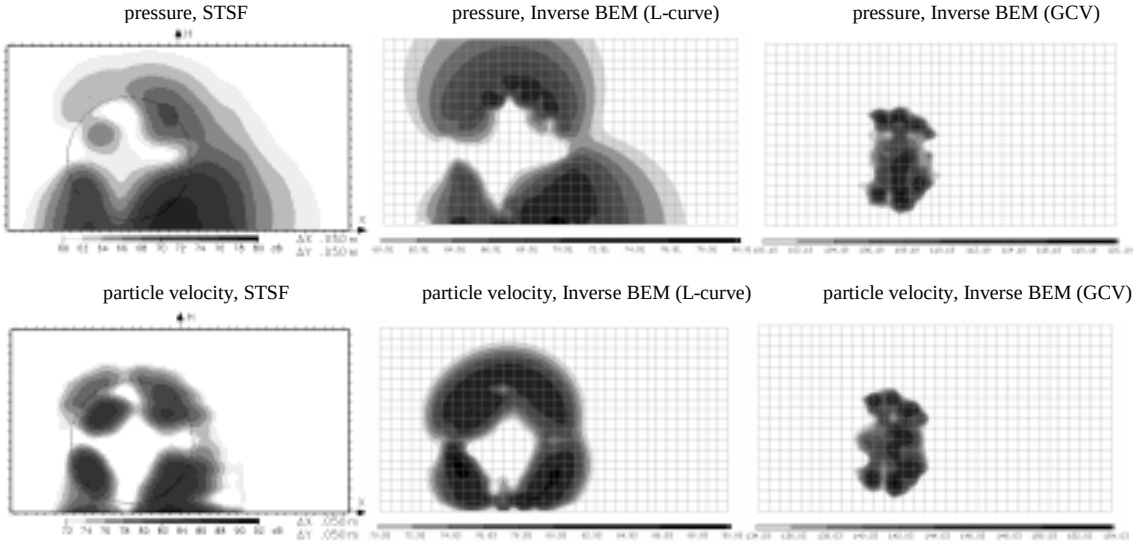

Figure 4. Reconstructed acoustic fields close to tyre-side for shaked tyre at 100 Hz.

In both figures, we see that the inverse BEM approach combined with the L-curve criterion provides a sound field picture which is more or less identical to the plot from STSF, both in terms of source localisation and absolute level. On the other hand, if we use the GCV method for computing the regularisation parameter, the solution becomes under-smoothed since the GCV method computes a regularisation parameter which is too small. This is not surprising, since GCV tends to fail if the error component of the measured field pressure vector is not predominantly white [4,6]. The L-curve criterion applied to each principal component gives rise to meaningful reconstructed sound fields, although we can not directly compare STSF and the inverse BEM as a different kind of filtering is inherent in each method. In particular, for the rolling tyre we see that the reconstructed particle velocity on the calculation plane shows a slightly higher level for inverse BEM than for STSF.
We conclude that the L-curve criterion for estimating the regularisation parameter in Tikhonov regularisation is more robust than the GCV method.

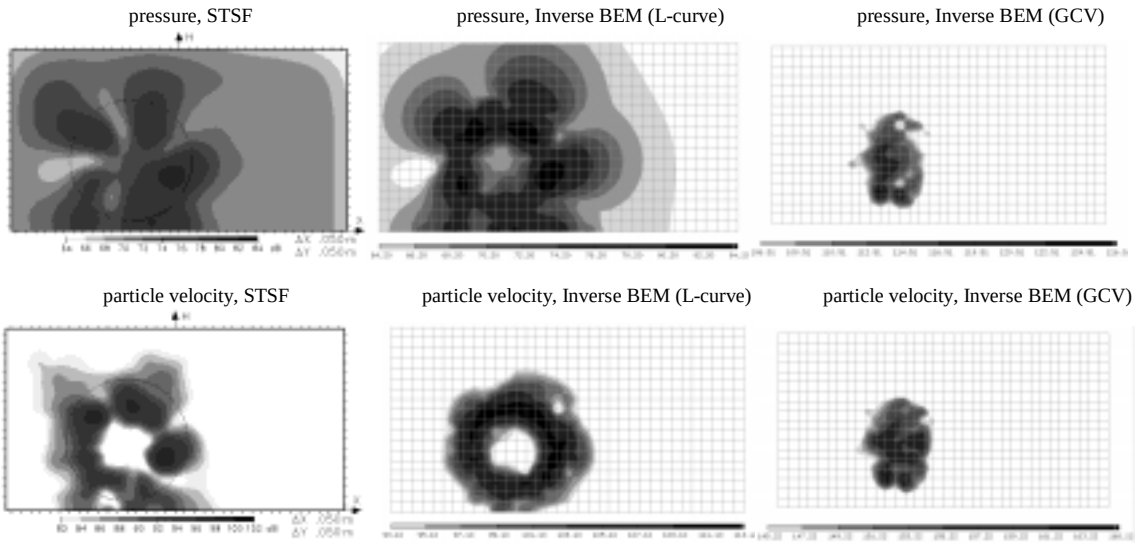

Figure 5. Reconstructed acoustic fields close to tyre-side for rolling tyre at 60 Hz.

References

1. J. Hald, “STSF – a unique technique for scan-based Near-field Acoustic Holography without restrictions on coherence”, Brüel & Kjær Technical Review no. 1 (1989).
2. W. A. Veronesi & J. D. Maynard, “Digital holographic reconstruction of sources with arbitrarily shaped surfaces”, J. Acoust. Soc. Am., **85**, 588-598 (1989).
3. M. R. Bai, “Application of BEM (boundary element method)-based acoustic holography to radiation analysis of sound sources with arbitrarily shaped geometries”, J. Acoust. Soc. Am., **92**, 533-549 (1992).
4. P. C. Hansen, *Rank-Deficient and Discrete Ill-Posed Problems*, SIAM, Philadelphia, 1997.
5. P. C. Hansen & D. P. O’Leary, “The use of the L-curve in the regularisation of discrete ill-posed problems”, SIAM J. Sci. Comput., **14**, 1487-1503 (1993).
6. A. Schuhmacher, “Sound source reconstruction using inverse sound field calculations”, Ph.D. Thesis, Dept. of Acoustic Technology, Technical University of Denmark, Report 77 (2000).